CMB polarization with the Bicep and Keck experiments

Michael Crumrine

April 5, 2017

1 Introduction

1.1 A Brief History of Inflation

The modern study of cosmology began in 1915 with Einstein's development of the general theory of Relativity [6]. By combining the Einstein Field Equations with the assumptions of a homogeneous and isotropic universe, Friedmann developed a cosmological model which forms the core of the standard model of cosmology[7]. Hubble's observations in the 1930s showed an expanding universe[8] providing the first evidence for a Big Bang origin. This was further supported by the detection of the Cosmic Microwave Background by Penzias and Wilson in 1965[11].

Increasing experimental precision revealed a uniform CMB and isotropic universe on scales exceeding the size of the horizon predicted by Friedmann cosmological models. In 1981 Guth suggested a small period of exponential expansion to solve these two problems. This theory of inflation has since seen further success in explaining the growth of cosmic structures and the lack of observed magnetic monopoles but has been criticized due to its need for fine-tuned initial conditions.

1.2 Origins of the CMB

One of the most successful predictions of inflation is the presence of a near uniform isotropic photon source known as the Cosmic Microwave Background (CMB).The CMB has the near uniform temperature spectrum of a 2.73K blackbody and is the source of the oldest photons in the universe. In the hot big bang, the early universe was an energetic plasma in which photons scattered continuously from free protons and electrons which prevented propagation over large distances. As the universe expanded, the temperature of this plasma decreased adiabatically until the free electrons and protons could combine to form neutral Hydrogen. After this era of recombination about 380,000 years after the big bang, the photons decoupled from the plasma and began free streaming through the universe, redshifting due to continued expansion. We observe these photons as a 2D "surface of last scattering".

2 Science with the CMB

2.1 Mapping the CMB

Precision cosmology experiments have shown that the CMB is not truly uniform. Results from COBE in 1992[4] showed the CMB to have a nearly isotropic temperature spectrum corresponding to a 2.73K blackbody but with fluctuations on the order of 10 μK. We examine these temperature perturbations with the spherical harmonics:

$$\delta T(\theta, \phi) = \sum_{m=-\ell}^{\ell} \sum_{\ell=0}^{\infty} a_{\ell m} Y_{\ell m}(\theta, \phi) \tag{1}$$

Although this decomposition is a powerful tool, the universe is isotropic only in a statistical sense and we therefore cannot predict any individual $a_{\ell m}$. We instead take an average over m for a given ℓ to form the angular power spectrum:

$$C_{ii_\ell} = \frac{1}{2\ell+1} \sum_{m=-\ell}^{\ell} \left\langle |a_{\ell m}|^2 \right\rangle \tag{2}$$

where ii refers to the type of anisotropy.

2.2 Polarization Anisotropies

In addition to the temperature anisotropies CMB photons are partially polarized due to Thompson scattering in a non-uniform temperature field. This CMB polarization was predicted at the $\approx 10\%$ level by Bond et al [5] and first detected by DASI in 2002 [10]. Polnarev [14] realized that an inflationary period would imprint an additional polarization signal on the CMB due to the production of gravitational waves.

This inflationary gravitational wave (IGW) signal is expected to be orders of magnitude fainter than the signal due to Thompson scattering and difficult to separate in the Stokes parameter space conventionally used in Electromagnetics when studying linearly polarized light. It was shown by Kamionkowski et al [9] that the polarization could instead be parameterized by a gradient (E-mode) and curl (B-mode) component. The signal produced by Thompson scattering occurs in the presence of a temperature quadrupole and follows the temperature gradients of the hot plasma at recombination and can therefore produce only E-modes. The tensor perturbations due to passing gravitational waves are not restricted in this way and can thus generate both E and B modes. The signal produced by these two methods is characterised by the tensor to scalar ration r. Figure 1 shows the theoretical power spectra of CMB perturbations in the ΛCDM standard model of Cosmology with the addition of an $r = 0.1$ IGW B-mode signal.

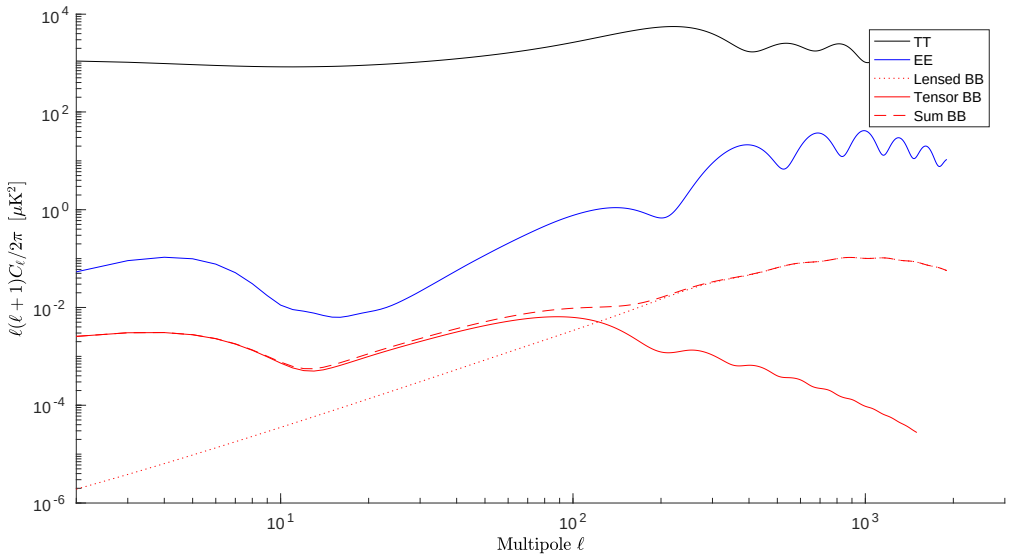

Figure 1: The CMB power spectrum of the ΛCDM standard model of cosmology as calculated by CAMB using parameters from Planck 2013. The temperature anisotropies (black) contain orders of magnitude more power than the E-mode (blue) and B-mode (red) polarization anisotropies. The BB spectrum is split into a lensing component (dotted) and a tensor component (solid) plotted at the $r = 0.1$ level.

2.3 Science with the CMB Power Spectrum

3 The Bicep and Keck Program

The Bicep/Keck experiments are a staged series of small aperture ground based telescopes which aim to produce extremely deep degree-scale polarization maps of the CMB. Each generation of receiver builds on the experience gained from the previous generation while pushing deeper in sensitivity. This progression is shown in Figure 2.

Bicep1 was deployed to the south pole in 2006 and used 98 feedhorn coupled bolometers observing at 100GHz and 150GHz. Over three observing seasons the strategies developed for observation, calibration and systematics control proved the efficacy of small aperture refractors for CMB polarization studies and established the leading upper bounds on inflation at $r < 0.70$ [1].

Building on the techniques developed with its predecessor, Bicep2 replaced Bicep1 in 2009. It exchanged feedhorn coupled bolometers for antenna-coupled transition edge sensor (TES)

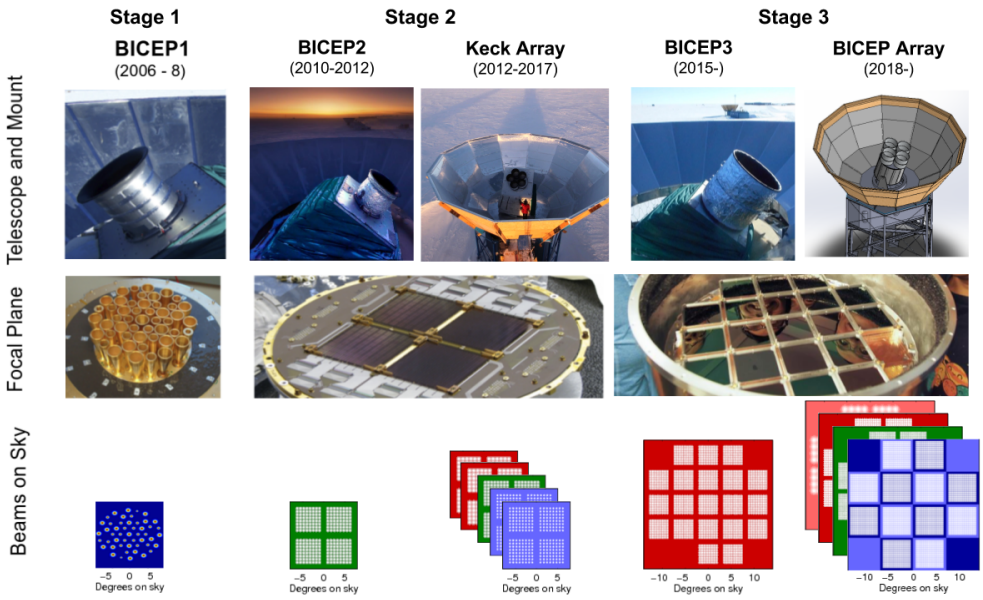

Figure 2: The progression of the Bicep/Keck program from Bicep1 to Bicep Array. The bottom row shows the beam patterns of the focal planes on the sky. With the exception of Bicep1 the focal plane colors correspond to band centers of: 35GHz - pink, 95GHz - red, 150GHz - green, 220 GHz - light blue, 270GHz - dark blue.

bolometer arrays developed at JPL which have been used in every subsequent telescope in the series. Concentrating its observing power at 150GHz, in March 2014 Bicep2 announced a detection of excess signal in its observing band consistent with an IGW signal of $r = 0.2$[2]. However, the interpretation of this excess as IGW signal relied heavily on models of polarized dust emission which had not been highly constrained at the time. Later that year new high frequency maps from the Planck experiment indicated that the dust models had underestimated polarized emission in the faintest sky regions [12]. A joint analysis with Planck and cross correlation between the Planck 353GHz and Bicep2 150GHz maps showed that a substantial part of the observed excess in Bicep2 was due to polarized dust emissions [3]. This joint analysis established a new upper limit of $r < 0.12$

Building on the observing power of Bicep2 the Keck Array deployed to the south pole in 2012 with five 150GHz receivers similar to Bicep2. These additional receivers confirmed the excess signal found with Bicep2 and contributed to the March 2014 results. In addition to

extending the Bicep2 survey depth at 150GHz the Keck array has extended observations into three other observing bands at 95GHz, 220GHz and 270GHz. The extension into other frequencies harnesses the Bicep/Keck program's proven capability to make deep maps to further constrain galactic foregrounds and refine the models of polarized dust emission. The Keck array is in its final observing season with four receivers in the 220GHz band and one at 270GHz.

In the fall of 2014 Bicep3 was deployed at the south pole to run concurrently with the Keck array. Bicep3 vastly expands the design of the Bicep2 instrument with a focal plane containing 2500 detectors in the 95GHz band, almost 10x the 288 detectors of a Keck style 95GHz receiver. Bicep3 serves as our prototype instrument leading to the eventual replacement of the Keck array with Bicep array.

The Bicep array is a funded experiment which will replace the Keck Array for multifrequency observations. Using the more powerful Bicep3 style receivers, Bicep array will field three receivers centered at 35GHz, 95GHz, and 150GHz along with a dual band 220/270GHz receiver. The new 35GHz receiver will heavily constrain galactic synchrotron radiation past the upper limits set by WMAP's 23GHZ band while the increased sensitivity at higher frequencies will allow for better constraints on dust emissions at frequencies closer to our other bands than the Planck 353GHz data.

4 Multifrequency Observations

CMB polarization experiments must be able to separate polarized foreground signals from those imprinted on the CMB. Although these signals can be minimized by selection of observing area their emissions must be constrained and accounted for. As shown by the 2014 joint analysis between Bicep2/Keck and Planck, constraints on these models have significant impact on the interpretation of any observed excess signal. By expanding observations into

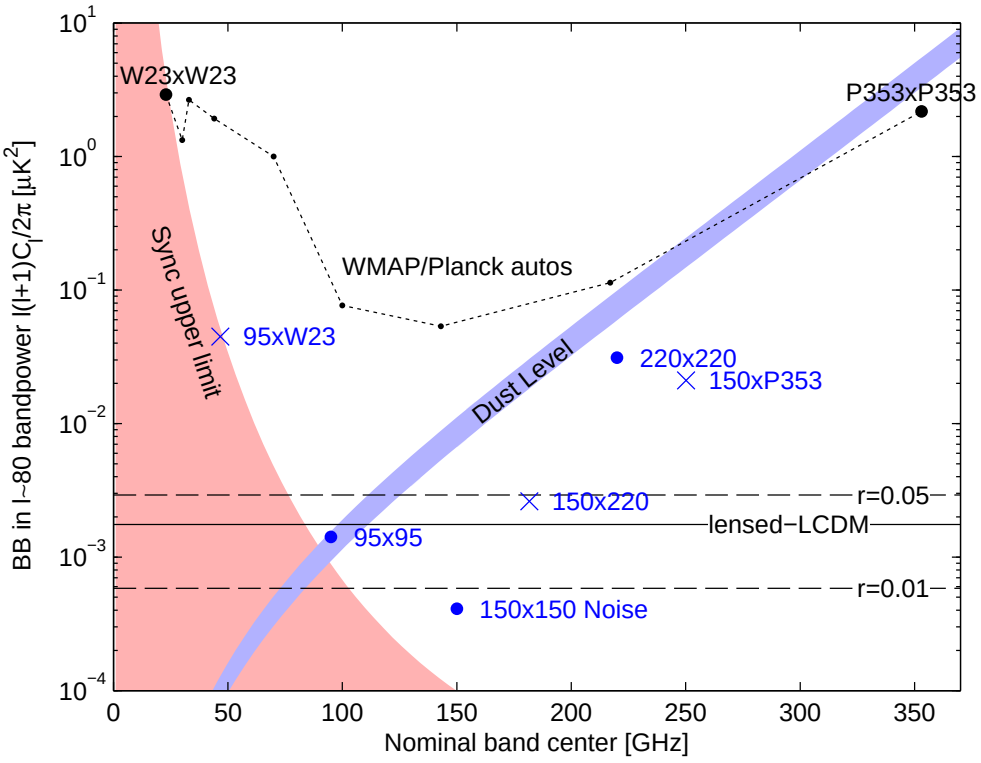

Figure 3

multiple frequencies, the Keck array has further constrained these dust emissions as well as emissions due to galactic synchrotron as shown in Figure 3.

4.1 Polarized Dust

Polarized emissions from galactic dust provide an excess BB signal on top of that expected from ΛCDM and gravitational lensing which (although low in power) are significant compared to the IGW signal. These emissions depend significantly on frequency, exhibiting a power law like dependence. As shown in Planck XXII [13] the spectral energy distribution of galactic dust can be described by a modified blackbody spectrum

$$I_d = A_d \nu^\beta B_\nu(T_d) \tag{3}$$

Where A_d is an amplitude at some frequency and $\beta_d > 0$ is the spectral index of dust emission and $B(T)$ is the standard blackbody spectrum. In order to fully constrain the dust signal we must complement this intensity spectrum with a description of the dust's spatial behavior

$$D_\ell \propto \ell^\alpha \tag{4}$$

where $D_\ell = C_\ell \frac{\ell(\ell+1)}{2\pi}$. The parameters in these equations model the dust contribution to polarization signal in our field. As Equation 3 shows this signal is brighter at higher frequencies. We therefore use the Planck 353GHz maps to set these dust parameters and extrapolate to our observed frequencies. This necessarily means that any uncertainty contained in the high frequency observations is magnified due to the power law behavior.

Figure 3 shows the noise uncertainty and signal levels the $\ell = 80$ bandpower where the IGW signal is expected to peak. The low 150x150 noise allows us to detect excess signal with high significance. However, the high P353xP353 noise as compared to dust signal does not provide significant enough constraining power to separate dust signal from potential IGW signal in the 150GHz band. The 220x220 point shows preliminary numbers from our 2015 observing season in which the Keck array operated with two 220GHz receivers and provides similar constraining power to the Planck 353GHz data while being closer to our main observing bands. Two additional 220GHz receivers were added for the 2016 observing season and observations at 270GHz will begin in the current 2017 season. These observations will allow us to produce continually improving constraints on dust in our field.

4.2 Galactic Synchrotron

An upper limit for an additional foreground signal is shown in Figure 3. Rather than increasing in intensity at higher frequencies, polarized emissions from galactic synchrotron

radiation are strongest at low frequencies. We model synchrotron emission intensity as

$$I_\nu = A_s \nu^{\beta_s} \tag{5}$$

where $\beta_s < 0$ describes the fall off in intensity with frequency and A_s is the amplitude. The angular power spectrum of galactic synchrotron follows the same form as dust (Equation 4). The points shown in Figure 3 mark the upper limit of synchrotron emissions as the noise level of current observations in these bands is not sufficient for detection. Models of the contribution due to synchrotron do not predict significant contamination at frequencies upwards of 150GHz due to the strong frequency dependence. **Add in new BK15 plot with BK16 prelim points**

4.3 Bicep Array

The Bicep Array experiment will leverage the technology used in Bicep3 and expand to a multifrequency array of receivers similarly to the expansion of the Keck array from Bicep2.

4.4 Detectors

Bicep Array will continue to use the dual polarization antenna coupled detector arrays developed for Bicep2. Each detector pixel consists of a large number of photolithographed orthogonal slot antennas optimized for their target wavelength. The summation of the incoming signal is eventually deposited into a resistor, changing the temperature of the coupled Transition Edge Sensor (TES). This produces a small change in temperature of the on-transition superconductive element which responds with a large change in resistance. This in turn leads to a small change in current which is amplified through a series array of Superconducting Quantum Interference Devices (SQUIDs) which are sensitive to extremely small changes in magnetic flux. This use of extremely sensitive superconducting sensors allows for detection

of extremely faint CMB signal but also requires high systematics control to avoid extraneous pickup from non-sky sources. The superconducting elements also require a carefully designed housing in order to reach their operating temperature of $273mK$.

4.5 Cryostat

The cryogenic operating temperature of the detectors in the Bicep/Keck experiments require carefully designed housing. Each generation of receivers builds on the experience gained from the previous generation to improve the design. The Bicep Array cryostats will consist of three concentric shells each cooled to progressively lower temperatures. These shells nominally sit at temperatures of 300K, 50K and 4K with the coolest being closest to the center.This progressive cold shielding significantly reduces the radiative power that is absorbed by the cooler stages which scales as $\Delta(T^4)$. The inclusion of absorptive filters on the 300K and 50K shells help to additionally reduce the out of band power transmitted down the optical axis.

-Widened 4K stage for extra baffling esp at 35GHZ -Same aperture size, throughput scales with num pixels -¿ frequency -Chart of pixel numbers and NETs per frequency across the receivers

References

[1] D. Barkats et al. "Degree-scale Cosmic Microwave Background Polarization Measurements from Three Years of BICEP1 Data". In: *apj* 783, 67 (Mar. 2014), p. 67. DOI: 10.1088/0004-637X/783/2/67. arXiv: 1310.1422.

[2] BICEP2 Collaboration et al. "Detection of B-Mode Polarization at Degree Angular Scales by BICEP2". In: *Physical Review Letters* 112.24, 241101 (June 2014), p. 241101. DOI: 10.1103/PhysRevLett.112.241101. arXiv: 1403.3985.

[3] BICEP2/Keck and Planck Collaborations et al. "Joint Analysis of BICEP2/Keck Array and Planck Data". In: *Physical Review Letters* 114.10, 101301 (Mar. 2015), p. 101301. DOI: 10.1103/PhysRevLett.114.101301. arXiv: 1502.00612.

[4] N. W. Boggess et al. "The COBE mission - Its design and performance two years after launch". In: *apj* 397 (Oct. 1992), pp. 420–429. DOI: 10.1086/171797.

[5] J. R. Bond and G. Efstathiou. "Cosmic background radiation anisotropies in universes dominated by nonbaryonic dark matter". In: *apjl* 285 (Oct. 1984), pp. L45–L48. DOI: 10.1086/184362.

[6] A. Einstein. "Die Feldgleichungen der Gravitation". In: *Sitzungsberichte der Königlich Preußischen Akademie der Wissenschaften (Berlin), Seite 844-847.* (1915).

[7] A. Friedmann. "Über die Krümmung des Raumes". In: *Zeitschrift fur Physik* 10 (1922), pp. 377–386. DOI: 10.1007/BF01332580.

[8] E. Hubble. "A Relation between Distance and Radial Velocity among Extra-Galactic Nebulae". In: *Proceedings of the National Academy of Science* 15 (Mar. 1929), pp. 168–173. DOI: 10.1073/pnas.15.3.168.

[9] M. Kamionkowski, A. Kosowsky, and A. Stebbins. "A Probe of Primordial Gravity Waves and Vorticity". In: *Physical Review Letters* 78 (Mar. 1997), pp. 2058–2061. DOI: 10.1103/PhysRevLett.78.2058. eprint: astro-ph/9609132.

[10] J. M. Kovac et al. "Detection of polarization in the cosmic microwave background using DASI". In: *nat* 420 (Dec. 2002), pp. 772–787. DOI: 10.1038/nature01269. eprint: astro-ph/0209478.

[11] A. A. Penzias and R. W. Wilson. "A Measurement of Excess Antenna Temperature at 4080 Mc/s." In: *apj* 142 (July 1965), pp. 419–421. DOI: 10.1086/148307.

[12] Planck Collaboration et al. "Planck intermediate results. XIX. An overview of the polarized thermal emission from Galactic dust". In: *aap* 576, A104 (Apr. 2015), A104. DOI: 10.1051/0004-6361/201424082. arXiv: 1405.0871.

[13] Planck Collaboration et al. "Planck intermediate results. XXII. Frequency dependence of thermal emission from Galactic dust in intensity and polarization". In: *aap* 576, A107 (Apr. 2015), A107. DOI: 10.1051/0004-6361/201424088. arXiv: 1405.0874.

[14] A. G. Polnarev. "Polarization and anisotropy induced in the microwave background by cosmological gravitational waves". In: *azh* 62 (Dec. 1985), pp. 1041–1052.